PROCEEDINGS OF SCIENCE

${}^{3}_{\Lambda}\mathrm{H}$ and ${}^{4}_{\Lambda}\mathrm{H}$ Lifetime, Yield and Directed Flow Measurements in Au+Au Collisions at $\sqrt{s_{\mathrm{NN}}} = 3$ GeV with the STAR Detector

Yue-Hang Leung[1]*, **for the STAR collaboration**

[1]*Nuclear Science Division, Lawrence Berkeley National Laboratory*
E-mail: yhleung@lbl.gov

The study of hyperon-nucleon (Y-N) interaction is of great interest in recent years because of its relation to high-density matter systems such as neutron stars. The presence of hyperons inside neutron stars would soften the equation of state. Hypernuclei, bound states of nucleons and hyperons, serve as a probe to study the Y-N interaction. The data from fixed target Au+Au collisions at $\sqrt{s_{\mathrm{NN}}} = 3$ GeV, taken in 2018 by the STAR detector, is ideal for studying the properties of light hypernuclei, such as ${}^{3}_{\Lambda}\mathrm{H}$ and ${}^{4}_{\Lambda}\mathrm{H}$, due to the large statistics and high production yield. In this talk, the lifetime of ${}^{3}_{\Lambda}\mathrm{H}$ and ${}^{4}_{\Lambda}\mathrm{H}$, the rapidity and centrality dependence of their yields in Au+Au collisions at $\sqrt{s_{\mathrm{NN}}} = 3$ GeV will be presented. The measured yield will be compared to measurements at other energies and theoretical models, and the physics implications will be discussed. We also report the first observation of the ${}^{3}_{\Lambda}\mathrm{H}$ and ${}^{4}_{\Lambda}\mathrm{H}$ directed flow in $5-40\%$ centrality. The directed flow of ${}^{3}_{\Lambda}\mathrm{H}$ and ${}^{4}_{\Lambda}\mathrm{H}$ are compared with those of the copiously produced particles such as p, Λ, d, t, ^{3}He and ^{4}He. These results will shed light on light hypernuclei production in heavy-ion collisions in high baryon density region.

International Conference on Critical Point and Onset of Deconfinement (CPOD2021)
15-19 March, 2021
Online

*Speaker.

1. Introduction

Hypernuclei provide access to the hyperon-nucleon (Y-N) interaction, which is an important ingredient in the equation of state of high-density nuclear matter, such as neutron stars. Measurements of the lifetime and Λ binding energy can provide information on the Λ-N potential.

The lightest known hypernucleus $^{3}_{\Lambda}$H has a very small Λ binding energy of a few hundred keV [1, 2]. Due to its loosely bound nature, the lifetime of the $^{3}_{\Lambda}$H is expected to be close to the free Λ lifetime. While recent ALICE measurements [3, 10] indicate a $^{3}_{\Lambda}$H lifetime to be consistent with the free Λ lifetime, HypHI [5] and STAR [11, 7] have reported $^{3}_{\Lambda}$H lifetime values less than that of the Λ, albeit with large uncertainties. More precise measurements are necessary to further our understanding of the structure of $^{3}_{\Lambda}$H and the Y-N interaction [9].

Measurements on the hypernuclei production yield can help us understand the production mechanisms of such loosely bound objects in heavy-ion collisions. At high energies, measurements of $^{3}_{\Lambda}$H production have been presented by ALICE [10] and STAR [11]. In Pb+Pb collisions at $\sqrt{s_{\mathrm{NN}}} = 2.76$ TeV, the measured $^{3}_{\Lambda}$H yields are consistent with both thermal model [12] and UrQMD [13] predictions. These calculations, however, diverge at lower energies, where the baryon density increases. The production mechanism of hypernuclei in this region is currently not well understood due to the lack of experimental data. Besides the production yield, anisotropic flow is an important observable that is sensitive to early stage collision dynamics [14]. Measurements of the hypernuclei yield and flow can help us understand the role of hyperons in the high baryon density region, as well as give insight into their production mechanisms.

In these proceedings, we present new results of the lifetime, yield, and directed flow of light hypernuclei $^{3}_{\Lambda}$H and $^{4}_{\Lambda}$H in Au+Au collisions at $\sqrt{s_{\mathrm{NN}}} = 3$ GeV, using data taken in 2018 by the STAR experiment at RHIC.

2. Experimental Setup and Dataset

These analyses utilize data from Au+Au collisions at $\sqrt{s_{\mathrm{NN}}} = 3$ GeV taken by the STAR experiment in 2018 using the fixed target setup [17, 18]. A single Au beam impinges on a 0.25 mm thick gold target located at the entrance of the Time Projection Chamber (TPC), about 200 cm away from its center. The minimum bias (MB) trigger condition is provided by the Beam-Beam Counters (BBC). The reconstructed primary vertex position along the beam direction is required to be within 2 cm of the nominal target position. In total, 2.8×10^{8} MB events were used in these analyses.

3. $^{3}_{\Lambda}$H and $^{4}_{\Lambda}$H Lifetime

$^{3}_{\Lambda}$H and $^{4}_{\Lambda}$H candidates are reconstructed via their two-body mesonic decay channels. Particle identification is based on the energy loss measurement by the TPC. The reconstructed hypernuclei candidates are shown in Fig. 1 (a,b). The background is estimated by rotating all π^{-} tracks in a given event and subsequently subtracted from the data. The number of signal counts is extracted using a bin counting method, and are shown as a function of $p_T - y$ in Fig. 1 (c,d). Good mid-rapidity coverage is attained in the $\sqrt{s_{\mathrm{NN}}} = 3$ GeV Au+Au collisions.

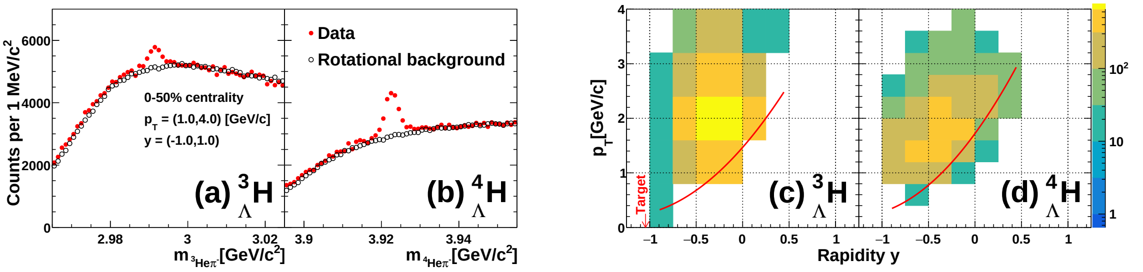

Figure 1: Invariant mass distributions of (a)^{3}He $-\,\pi$ and (b)^{4}He $-\,\pi$ pairs reconstructed from data are shown on the left. Black circles represent the background constructed by using pion tracks rotated by 180 degrees. The transverse momentum (p_T) versus the rapidity (y) for reconstructed (c)$^{3}_{\Lambda}$H and (d)$^{4}_{\Lambda}$H are shown on the right.

The number of $^{3}_{\Lambda}$H and $^{4}_{\Lambda}$H counts in the data are extracted as a function of $L/\beta\gamma$, where L is the decay length, β is the velocity and γ is the Lorentz factor. The raw signal counts in each $L/\beta\gamma$ interval are subsquently corrected by the acceptance and reconstruction efficiency using GEANT3 [15]. The corrected Λ, $^{3}_{\Lambda}$H, and $^{4}_{\Lambda}$H $dN/d(L/\beta\gamma)$ are all well described by exponential functions. The lifetime is extracted by fitting an exponential function to the corrected $dN/d(L/\beta\gamma)$ distribution. For the case of Λ, the extracted lifetime is 265 ± 2 ps, consistent with PDG value [16].

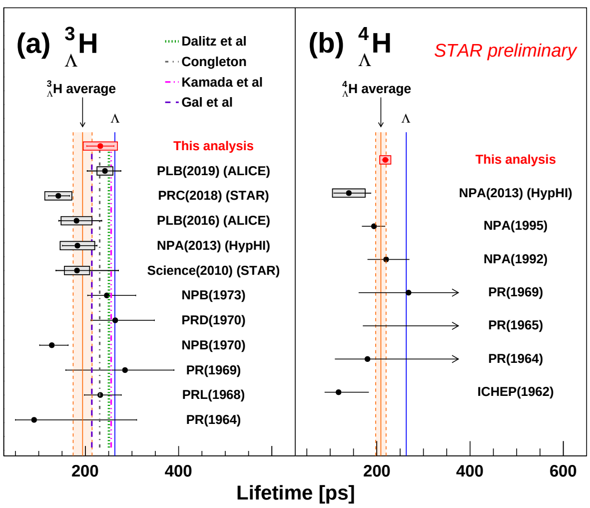

Figure 2: $^{3}_{\Lambda}$H (a) and $^{4}_{\Lambda}$H (b) measured lifetimes, compared to previous measurements, theoretical calculations and the free Λ lifetime. The experimental average lifetimes and the corresponding uncertainty are also shown as orange bands.

We considered four sources of systematic uncertainties, arising from (1) imperfect description of topological variables in the simulations, (2) imperfect knowledge of the true kinematic distribution of the hypernuclei, (3) the tracking efficiency of the TPC, and (4) the background subtraction method. Their contributions are estimated by varying topological cuts used in the analysis, the MC hypernuclei p_T–y distributions, the TPC track quality selection criteria and the background subtraction method. These uncertainties are assumed to be uncorrelated and added in quadrature.

The lifetimes of $^{3}_{\Lambda}$H and $^{4}_{\Lambda}$H are measured to be $\tau_{^{3}_{\Lambda}\mathrm{H}} = 232 \pm 29(stat) \pm 37(syst)$ ps and $\tau_{^{4}_{\Lambda}\mathrm{H}} = 218 \pm 8(stat) \pm 12(syst)$ ps respectively. The new results are shown in Fig. 2, and are compared to previous measurements and theoretical calculations. Both measurements are consistent with previous measurements, and the global averages are shown as orange shaded bands. For $^{3}_{\Lambda}$H, the global average is $(74 \pm 8\%)$ of the free Λ lifetime, consistent with calculations incorporating effects from pion final state interactions [8]. The presented $^{4}_{\Lambda}$H lifetime is the most precise measurement to date, providing more stringent constraints to theoretical models.

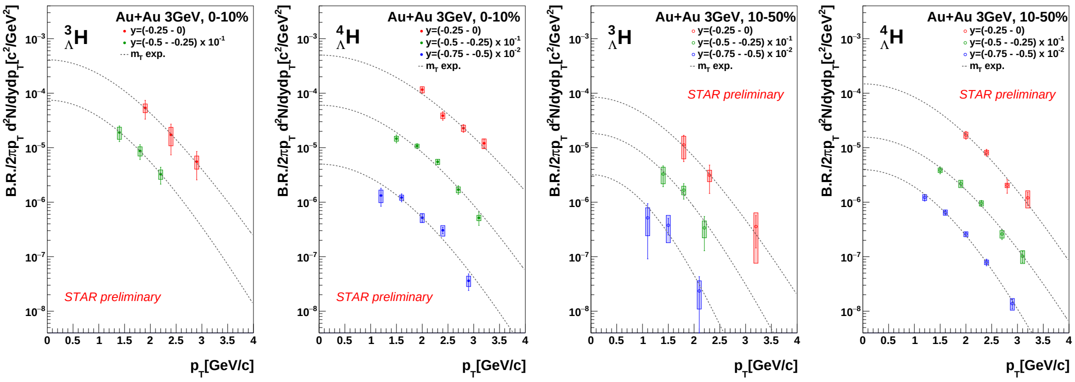

Figure 3: p_T spectra for $^{3}_{\Lambda}$H and $^{4}_{\Lambda}$H in (left) $0-10\%$ and (right) $10-50\%$ Au+Au collisions at $\sqrt{s_{\mathrm{NN}}} = 3$ GeV in different rapidity selections. The dotted lines represent fits using the m_T exponential function to the data points.

4. $^{3}_{\Lambda}$H and $^{4}_{\Lambda}$H Yield

$^{3}_{\Lambda}$H and $^{4}_{\Lambda}$H yields are also extracted in different p_T, rapidity and centrality selections. The p_T and rapidity differential yield in $0-10\%$ and $10-50\%$ centrality collisions are shown in Fig. 3.

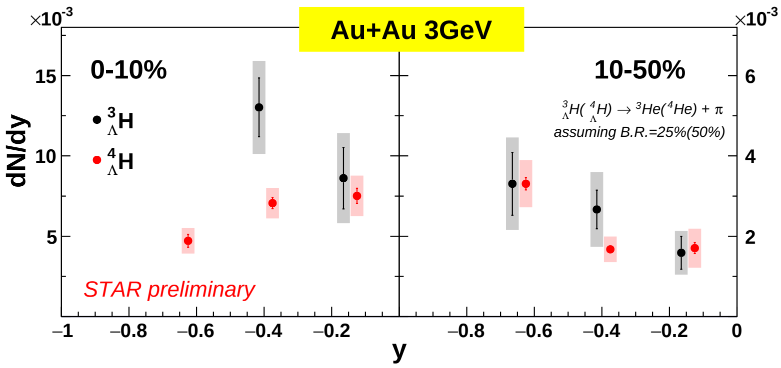

Figure 4: dN/dy as a function of rapidity y for $^{3}_{\Lambda}$H (black) and $^{4}_{\Lambda}$H (red) for (left) $0-10\%$ centrality and (right) $10-50\%$ centrality Au+Au collisions at 3 GeV.

To estimate the p_T integrated yield, the data are extrapolated down to $p_T = 0$. Besides the aforementioned systematic uncertainties, uncertainties from extrapolation to the unmeasured regions are considered; different functional forms are used for the extrapolation to estimate this uncertainty. The p_T integrated dN/dy as a function of rapidity are shown in Fig. 4. For $^{4}_{\Lambda}$H, we observe that the trend of the rapidity distribution changes from concave downwards to upwards from $0-10\%$ to $10-50\%$ centrality. This change is likely related to the change in the collision geometry, for example, spectators are expected to play a larger role in non-central collisions.

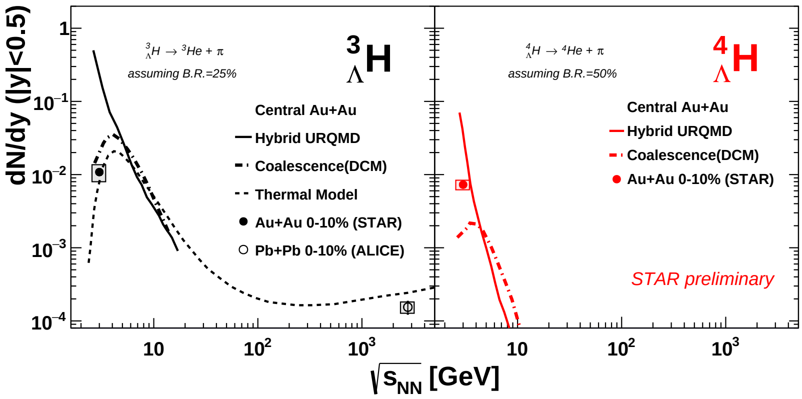

Figure 5: (left) $^{3}_{\Lambda}$H and (right) $^{4}_{\Lambda}$H yields at $|y| < 0.5$ as a function of beam energy in central heavy-ion collisions. The symbols represent measurements while the lines represent different theoretical calculations [12, 13].

In Fig. 5, the mid-rapidity ($|y| < 0.5$) $^{3}_{\Lambda}$H and $^{4}_{\Lambda}$H yields in $0-10\%$ $\sqrt{s_{NN}} = 3$ GeV Au+Au collisions are shown as a function of beam energy, and are compared measurements at different energies and theoretical calculations. The thermal model calculation [12], which incorporates canonical suppression at lower energies, can describe the $^{3}_{\Lambda}$H yield over few orders of magnitude of beam energy. Although the coalescence model [13] can describe the $^{3}_{\Lambda}$H yield at $\sqrt{s_{NN}} = 3$ GeV, it underestimates the $^{4}_{\Lambda}$H yield. On the other hand, hybrid URQMD model [13] overestimates both the $^{3}_{\Lambda}$H and $^{4}_{\Lambda}$H at $\sqrt{s_{NN}} = 3$ GeV. These measurements provide new insight to hypernuclei production in the high baryon density region.

5. $^{3}_{\Lambda}$H and $^{4}_{\Lambda}$H Directed Flow

The event plane method is used to extract the directed flow v_1 of $^{3}_{\Lambda}$H and $^{4}_{\Lambda}$H. The 1$^{\text{st}}$-order event plane angle is measured using the event plane detector, located at backward rapidity $(-5.3 < \eta < 2.6)$. The event plane resolution is estimated using the three subevent method [19]. For $^{3}_{\Lambda}$H, the 3-body decay channel $^{3}_{\Lambda}\text{H} \rightarrow \text{d} + \text{p} + \pi$ is also utilized to enhance the statistical precision. The $^{3}_{\Lambda}$H and $^{4}_{\Lambda}$H v_1 as a function of rapidity are shown in the left panels of Fig. 6. The p_T windows used for v_1 extraction for $^{3}_{\Lambda}$H and $^{4}_{\Lambda}$H are $(1.0-2.5)$ and $(1.2-3.0)$ GeV$/c$, respectively. A linear fit through the origin to the data is used to extract the slope dv_1/dy. The v_1 slope as a function of mass is shown in the right panel of Fig. 6. Only statistical uncertainties are shown. It is observed that the v_1 of light nuclei follows a mass scaling behavior. In addtion, the v_1 of hypernuclei are similar to that of light nuclei with the same mass number. These observations are qualitatively consistent with hypernuclei formation through the coalescence of hyperons and nucleons.

6. Summary

In conclusion, we have presented new measurements of $^{3}_{\Lambda}$H and $^{4}_{\Lambda}$H lifetime, yield and directed flow, using data taken by the STAR detector from Au+Au collisions at $\sqrt{s_{NN}} = 3$ GeV. The hypernuclei lifetimes are measured to be $\tau_{^{3}_{\Lambda}\text{H}} = 232 \pm 29(stat) \pm 37(syst)$ ps and $\tau_{^{4}_{\Lambda}\text{H}} = 218 \pm 8(stat) \pm$

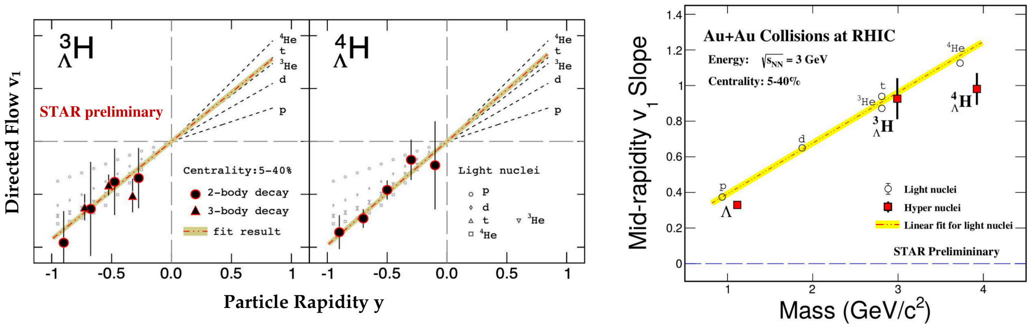

Figure 6: (left) ${}^3_\Lambda$H and ${}^4_\Lambda$H v_1 as a function of rapidity. The red line represents a linear fit. (right) ${}^3_\Lambda$H and ${}^4_\Lambda$H mid-rapidity v_1 slope as a function of mass. The dv_1/dy for light nuclei is shown for comparison.

$12(syst)$ ps. Both measurements are consistent with previous results. For ${}^3_\Lambda$H, the result is consistent with theoretical calculations incorporating pion final state interactions. These measurements can provide stonger constraints to model calculations. We also present the dN/dy of ${}^3_\Lambda$H and ${}^4_\Lambda$H in $0-10\%$ and $10-50\%$ 3 GeV Au+Au collisions. Thermal model incorporating canonical suppression for strangeness reproduces the mid-rapidity ${}^4_\Lambda$H yield. Coalescence model calculations also reproduce the ${}^3_\Lambda$H yield, but underestimate the ${}^4_\Lambda$H yield. Finally, we present the first observation of the directed flow of ${}^3_\Lambda$H and ${}^4_\Lambda$H in $5-40\%$ centrality Au+Au collisions at $\sqrt{s_{NN}} = 3$ GeV. We find that the mid-rapidity v_1 slope of ${}^3_\Lambda$H and ${}^4_\Lambda$H are similar to those of light nuclei with similar mass. This indicates that hypernuclei v_1 approximately follow baryon mass scaling, which is qualitatively consistent with hypernuclei formation through the coalescence of hyperons and baryons.

References

[1] M. Juric et al., Nucl. Phys. B **52**, 1(1973).

[2] J. Adam et al. (STAR), Nature Phys. **16**, 409(2020)

[3] S. Acharya et al. (ALICE), Phys. Lett. B **797**, 134905374(2019)

[4] J. Adam et al. (ALICE), Phys. Lett. B **754**, 360(2016)

[5] C. Rappold et al., Nucl. Phys. A **913**, 170(2013)

[6] B. I. Abelev et al. (STAR), Science **328**, 58(2010)

[7] L. Adamczyk et al. (STAR), Phys. Rev. C **97**, 054909382(2018)

[8] A. Perez-Obiol, D. Gazda, E. Friedman, and A. Gal, Phys. Lett. B **811**, 135916(2020)

[9] A. Gal, E. V. Hungerford, and D. J. Millener, Rev. Mod Phys. **88**, 035004(2016)

[10] J. Adam et al. (ALICE), Phys. Lett. B **754**, 360(2016)

[11] B. I. Abelev et al. (STAR), Science **328**, 58(2010)

[12] A. Andronic, P. Braun-Munzinger, J. Stachel, and H. Stocker, Phys. Lett. B **697**, 203 (2011)

[13] J. Steinheimer et al, Phys. Lett. B **714**, 85360(2012)

[14] C.M. Hung and E. Shuryak, Phys. Rev. Lett. **75**, 4003 (1995)

[15] R. Brun, F. Bruyant, M. Maire, A. C. McPherson, and P. Zanarini (1987)

[16] P.A. Zyla et al. (Particle Data Group), Prog. Theor. Exp. Phys. 2020, **083C01** (2020) and 2021 update

[17] M. S. Abdallah et al. (STAR), arXiv:2108.00908

[18] M. S. Abdallah et al. (STAR), arXiv:2108.00924

[19] J. Jia et al, Phys. Rev. C **96** (2017) 3, 034906